

Prospects for the detection of GRBs with HAWC

I. Taboada^a, R.C. Gilmore^b

^a*School of Physics and Center for Relativistic Astrophysics, Georgia Institute of Technology, Atlanta, GA USA*

^b*Santa Cruz Institute for Particle Physics. University of California. Santa Cruz, CA USA.*

Abstract

The observation of Gamma Ray Bursts (GRBs) with very-high-energy (VHE) gamma rays can provide understanding of the particle acceleration mechanisms in GRBs, and can also be used to probe the extra-galactic background light and place constraints on Lorentz invariance violation. We present prospects for GRB detection by the ground-based HAWC (High Altitude Water Cherenkov) gamma-ray observatory. We model the VHE spectrum of GRBs by extrapolating observations by Fermi LAT and other observatories to higher energies. Under the assumption that only e-pair production associated with extra-galactic background light is responsible for high-energy cutoffs in the spectrum, we find that HAWC will have a detection rate as high as 1.65 GRBs/year. Most of the sensitivity of HAWC to GRBs is derived from short-hard GRBs during the prompt phase. We explore the possibility of universal high-energy cutoffs in GRB spectra and find that the GRB detection rate by HAWC should be at least half of this figure as long as the typical intrinsic cutoff is above 200-300 GeV in the rest frame.

Keywords: Gamma-ray burst, air shower, High Altitude Water Cherenkov Observatory, gamma rays

1. Introduction

Gamma Ray Bursts (GRBs) are among the most powerful events in the Universe, and have been the subject of observational studies from radio to multi-GeV energies. Fermi LAT has shown that GRBs are able to produce photons up to observed energies of 94 GeV (≈ 126 GeV after redshift correction) for GRB 130427A [1]. It is unknown up to what energy the spectrum extends, as present-day observations are limited by effective area, in the case of space-based instruments, and by slewing constraints and energy threshold for ground-based Imaging Air Cherenkov Telescopes. Studying the spectrum beyond 10 GeV is of interest in understanding GRB mechanisms themselves, and also allows us to probe cosmological phenomena such as the extra-galactic background light (EBL) and it may be used to constrain Lorentz invariance violation. The GRB proper, or prompt emission, is detected in the keV-MeV band by space-borne instruments such as Fermi-GBM [2] and Swift-BAT [3]. There are at least two known classes of GRBs, short-hard GRBs and soft-long GRBs. The short-hard variety (sGRBs) have durations of less than 2 s and a peak of νF_ν at Earth is at ~ 1 MeV. SGRBs are believed to be the result of the merger of two compact objects [4, 5], such as two neutron stars or a neutron star and a solar mass black hole. Long-soft GRBs (LGRBs) last more than 2 s and the peak of νF_ν is at ~ 50 keV. Core collapse supernova type Ic are believed to be the progenitors of LGRBs and coincidences of the two have been observed [6]. For both types of GRBs, emission is believed to happen in highly relativistic narrow jets that point in the direction of Earth.

In this paper we will show that the GRB detection rate by the extended air shower array detector HAWC may be as high as 1.65 GRBs per year, assuming that the spectrum is only cutoff by EBL attenuation, and that short GRB detection over the lifetime of the instrument is likely as long as intrinsic spectral cutoffs are not typical below ≈ 150 GeV in the rest frame. The most important energy range for detection by HAWC is in 50 GeV - 500 GeV range.

*Corresponding author: itaboada@gatech.edu

Satellites with instruments sensitive to hard gamma-rays, such as CGRO and Fermi, have extended the observations from 30 MeV to tens of GeV. GRB 130427A [1] that was observed up to 94 GeV, or 126 GeV once corrected for redshift, shows that GRBs are capable of producing very-high-energy (VHE) photons. As of May 2013, seven GRBs have been observed above 10 GeV [7, 8, 9, 10, 11, 1].

The keV-MeV burst spectrum is usually well described by the Band function [12]. At higher energies, Fermi LAT has shown that additional non-Band components are needed for every single high signal to noise ratio GRB [11]. This additional component can be a hard power law with no obvious high energy cutoff, such as GRB 090510 [8]. It can also be a cutoff in the high energy extension of the Band function such as GRB 100724B [11]. Or it can be a hard power law with a high energy cutoff, such as GRB 090926 [11]. For LGRBs, all cases of additional components have been observed in high signal/noise GRBs, but for sGRBs, only an additional power law with no cutoff has been observed. The number of bursts with high signal to noise ratio is low [11], thus, the relative frequency of each type of additional component is fairly uncertain.

Satellites are ideal platforms for GRB observations above 100 MeV and below a few tens of GeV. However, because of their limited size, and because spectra fall off as a power law of energy, they are not appropriate to extend the observations to even higher energies. The >30 GeV study of the non-Band components is of interest in several respects. A cutoff in the spectrum may be indicative of e-pair production at the source and thus a measurement of the Lorentz boost factor of the jet. A cutoff is also possible due to EBL attenuation. For redshifts lower than $z \approx 1$, the EBL cutoff energy is $\gtrsim 100$ GeV and probably would not be observable by Fermi-LAT or other space borne instruments. Observation of the >30 GeV spectrum may also be used to constrain Lorentz invariance violation and to model particle acceleration in GRBs. Finally spectral and temporal information of >30 GeV emission may help constrain GRB models.

Ground based detectors are ideal for >30 GeV studies of GRBs. Two techniques are available: Air Cherenkov Telescopes (IACTs) and Extended Air Shower arrays (EAS). IACTs have better sensitivity both due to larger effective area and better background rejection. However IACTs have limited field of view, which requires them to slew fast after an alert to observe GRBs. The best slewing time for VERITAS is ≈ 100 s [13], which results in observations that are in the early afterglow phase. The other disadvantage is that IACTs operate only in good weather, at night, with no or limited moon light. The duty cycle of IACTs is 10-15% and bright GRBs, that may result in >30 GeV observations are rare events. Finally, IACTs need GRBs to have a small localization error, so as guarantee that the search area fits into the field of view. EAS arrays have lower sensitivity, but they have the advantage of very high duty cycle (over 95%) and very large instantaneous field of view (nominally 2 sr) so they are able to catch rare bright GRBs. Furthermore, the wide field of view allows EAS arrays to study GRBs with a localization error of several degrees, as is often the case for GRBs reported by Fermi GBM.

A previous study [14] of the prospects for the detection of GRBs by CTA, a proposed 3rd generation IACT, found that CTA will be mostly sensitive to LGRBs in the afterglow phase, with a detection rate of 0.5-2 GRBs/yr (depending on detector configuration, GRB satellite alert rate, and high energy spectral model applied) assuming that the only cutoff in the high-energy spectrum is due to EBL [14]. In the current publication we will follow a similar method as used for CTA, but applied to HAWC.

2. HAWC

The HAWC (High Altitude Water Cherenkov) observatory is an EAS array in construction in Central Mexico at 4100 m asl. Once completed it will consist of 300 water tanks of 7.3 m in diameter and 4.5 m of depth. Each tank will contain three 8" PMTs and one high quantum efficiency 10" PMT. HAWC is sensitive to GRBs with two modes of operation, the *main DAQ* and the *scaler DAQ*. The main DAQ operates by measuring the arrival time of the particle shower front product of the interaction of a high energy gamma ray in the upper atmosphere. Angular resolution for energies relevant to GRBs is $\approx 1^\circ$ and energy resolution is very poor, as the detector operates near the threshold [15]. The scaler DAQ operates in the single particle technique [16], in which a large transient fluence of gamma rays is found as a statistical excess in the count rate of all PMTs in the detector combined. The scaler DAQ does not provide localization and has not energy resolution. The energy response of both the main DAQ and scaler DAQ are different, thus the spectrum of a jointly observed GRB may be constrained [15]. Once operational HAWC will be the EAS array with the

best sensitivity to GRBs and would be able to detect historical GRBs, such as 090902B and 090510 if they fall in its field of view [15].

The publication by HAWC that describes the sensitivity to GRBs [15], excludes the central 10° PMT. The results presented here use the effective area presented in the HAWC publication. We interpolate both in zenith and energy to obtain the effective area for any zenith in the range 0 to 40° and any energy from 12 GeV to 1 TeV for the main DAQ. For the scaler DAQ, the zenith range is the same but energy is interpolated in the range 1 GeV to 1 TeV, reflecting better sensitivity to softer spectra provided by the scaler system. We use the background parameterization of both the main DAQ and the scaler DAQ presented in the HAWC publication [15]. For the main DAQ we use a trigger threshold of 30 PMTs, since the HAWC collaboration has indicated it believes it can operate at a very low threshold [15].

As suggested in the HAWC publication we use a search circle of 1.1° for the main DAQ. As we indicated before, HAWC and other EAS arrays can study GRBs with poor localization. For GRBs reported by Fermi GBM alone, the localization uncertainty is $\approx 10^\circ$. HAWC can tile the sky with ≈ 80 search regions, corresponding to applying a search trials factor of ≈ 80 . In our simulation of sGRBs we find that the background in 2 seconds for the main DAQ ranges from 2 to 16 events with an average of 7.5 events. The background rate in our calculation is exclusively a function of zenith angle. The number of counts needed for a 5σ excess over a expected 7.5 background events is 26 counts - or 18.5 signal events (the p-value for 26 counts is 2.9×10^{-8} , but 25 counts is below the 5σ threshold). With a trials factor of 80, the number of counts needed would be 28, or 20.5 signal counts. Tiling the sky results in a loss of sensitivity of $\approx 10\%$ with respect to knowing the GRB location with high precision. This simplistic calculation shows that we can ignore the trial factors for tiling the sky in searching for GRBs with poor localization. It should be further noted that bright Fermi GBM bursts have typically better localization than dim ones and as the simulations that we present here show, GRBs that can be detected by HAWC are expected to be bright as observed by Fermi GBM.

The sensitivity of HAWC to GRBs is in part a function of the time window in which VHE emission is searched. The shorter the burst the better sensitivity as the background is reduced. In our calculations here we simplistically assume that the search will be performed in a window of width T_{90} as measured by Fermi GBM for LGRBs and in a fixed window of 2 s for sGRBs.

3. Modeling of VHE emission by GRBs

We have built a model for >1 GeV spectrum for GRBs and simulated a large number of pseudo-GRBs. We assume that HAWC observations are triggered by Fermi GBM. While there are other satellites that contribute to a significant number of GRB alerts each year, notably Swift BAT, we find that bright GRBs are the most likely to result in detections by HAWC. Thus it is more important for HAWC to follow a very wide field of view space borne detector such as Fermi GBM, instead of a more sensitive detector such as Swift BAT. The study of CTA GRB detection rate found that most detections would be triggered by Swift because, as opposed to Fermi GBM, it provides localizations of an arcminute or better.

We model the > 1 GeV emission assuming an additional power law component that extends up to 1 TeV (at Earth) and is cutoff exclusively by EBL. The simulation samples from fits to the distribution of redshift for both LGRBs and sGRBs. The spectrum above 1 GeV is assumed to be a power law. We normalize the power law given a relationship found between the fluences measured by Fermi GBM and Fermi LAT. Correlations among parameters that describe GRBs are not simulated.

The simulated spectrum is folded with HAWC's interpolated effective area. The sensitivity for each GRB is found taking into account the parameterized background. To account for other potential sources of cutoff other than EBL we complement the calculation described above with a similar one that adds a universal Heaviside cutoff in the GRB self frame ranging from 100 GeV to 500 GeV.

3.1. > 1 GeV spectrum

Observations by Fermi LAT and Fermi GBM show a correlation between the low energy fluence, reported in the 10 keV - 10 MeV band (henceforth the GBM band), and the high energy fluence, reported in the

100 MeV - 10 GeV band (henceforth the LAT band). There is significant scatter around this correlation, and in the case of sGRBs, only 2 GRBs, 081024B and 090510, provide a hint of the correlation [11]. The duration (T_{90}) as measured in the two energy bands is different, and the LAT observation is usually delayed with respect to the GBM observation. However the correlation of fluences remains true even if the LAT observations are restricted to GBM's T_{90} . Indeed, approximately half of the fluence in the LAT band is produced in coincidence with GBM's T_{90} [11]. For LGRBs, the LAT fluence in GBM's T_{90} is approximately 10% the GBM fluence and for sGRBs this ratio is over 100% [11]. A critical ingredient in our model is the selection of 100% (10%) fluence ratio for sGRBs (LGRBs).

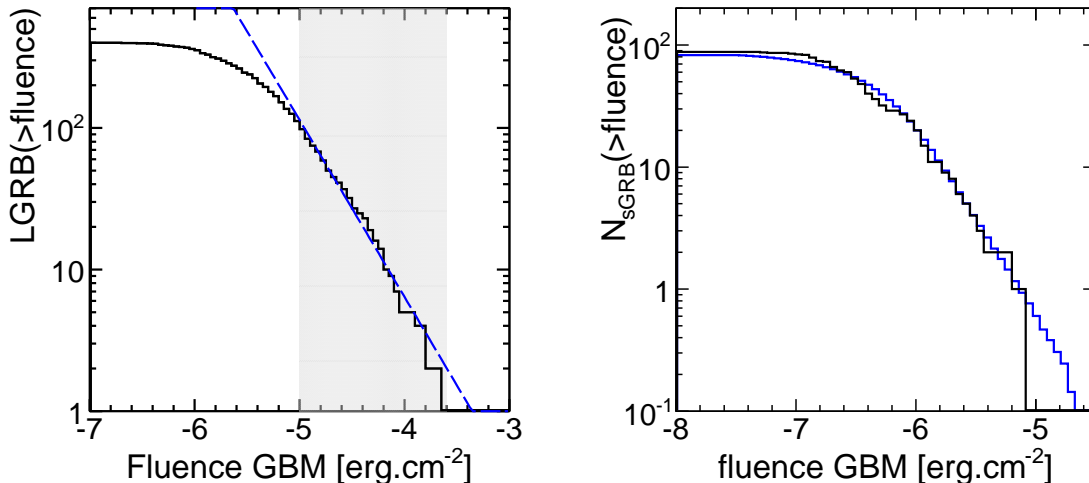


Figure 1: Cumulative distribution of GRBs as a function of fluence measured by Fermi GBM in the 10 keV - 10 MeV band [17]. The distribution of LGRBs (left) has been fitted with a power law using the shaded region. For sGRBs (right) a more elaborate function has been fitted to the data. At high fluence the cumulative distribution of sGRBs is also well described by a power law.

We have parameterized Fermi GBM's fluence using the data from the 2 year GBM catalog [17]. Fig. 1 shows that the cumulative distribution of bright GRBs are well described by a power law. At low fluences the effect of GBM's trigger becomes important. In our model, bright GBM GRBs are those that result in HAWC observations, thus a very detailed description of Fermi GBM's trigger is not critical. The Fermi GBM trigger would naturally introduce a correlation between GBM fluence and GBM T_{90} . As HAWC will observe GRBs mostly above the GBM trigger, we can ignore this correlation.

For LGRBs we have fitted the distribution of the number of GRBs above a given GBM fluence in the range $1 \times 10^{-5} - 2.5 \times 10^{-3} \text{ erg}\cdot\text{cm}^{-2}$. We find that the LGRB distribution is well described by a power law of index -1.5. This index is consistent with previous observations including those by Fermi GBM [17]. We normalize the rate of LGRBs in Fermi GBM by observing that there are 29 LGRBs in the 2 year GBM catalog above fluence of $3 \times 10^{-5} \text{ erg}\cdot\text{cm}^{-2}$. Figure 1 shows the distribution of GBM fluences for LGRBs as well as the power law fit. For fluences below $\approx 1 \times 10^{-5} \text{ erg}\cdot\text{cm}^{-2}$, the power law does not account for trigger effects of Fermi GBM. A result of the calculations that we present here is that only 3% of the GRBs detectable by HAWC would have a GBM fluence below $1 \times 10^{-5} \text{ erg}\cdot\text{cm}^{-2}$.

We have followed a similar procedure to parameterize the fluence of sGRBs. For sGRBs that are well above the GBM threshold, we also find that a power law of index -1.5 also provides a good description. However we find a larger fraction of sGRBs with fluence near the GBM threshold can result a detection by HAWC. A simple threshold on $F_{GBM}/\sqrt{T_{90}}$, where F_{GBM} is the GBM fluence does not accurately describe the detector threshold. The GBM trigger probably is better described in terms of the peak flux from a sGRB, and thus it depends on the details of the lightcurve of the sGRBs. To avoid unnecessary complexity we instead parameterize the cumulative distribution of sGRBs above a certain GBM fluence including an

arbitrary function to represent the trigger and we ignore the correlation with GBM's T_{90} . This is a valid approach as the calculations presented here assume that HAWC performs its search in a fixed 2 s window for sGRBs. Figure 1 shows the cumulative sGRBs above a given GBM fluence along with the cumulative distribution of simulated pseudo-GRBs that follow the fitted function. To normalize the absolute rate of sGRBs in Fermi GBM, we note that in the 2 year Fermi GBM catalog [17] there are 20 sGRBs above a fluence of 1×10^{-6} erg.cm $^{-2}$.

For both LGRBs and sGRBs we have tested values of the index that differ from -1.5 to describe the cumulative rate of GRBs as a function of GBM fluence. Using a value of -1.25 results in a detection rate that changes by only 3%.

We assume that every single simulated pseudo-GRB, of both long-soft and short-hard type, has an additional power law component. This is already in contradiction with observations by LAT of high signal to noise GRBs [11]. At the very minimum it is in contradiction for LGRBs. Therefore our present calculations for LGRBs are an over estimate of the rate in HAWC. There are only a handful of high signal to noise ratio GRBs in LAT data, and these are not clearly identified as such in the 3 year Fermi LAT GRB catalog [11]. However we estimate that one third to one half of the high signal to noise ratio LAT LGRBs have an additional power law with no indication of cutoff in the LAT band. For LGRBs with an additional power law in LAT, the central value of the spectral index is -2 so we assume this value in our simulations.

Only 2 sGRBs have high signal to noise ratio in LAT, GRB 081024B [18] and 090510 [11]. They both have a very hard additional component of index -1.6. Evidence for additional power law components have been seen on other GRBs for which Fermi LAT observations are not available. The three brightest sGRBs in GBM, GRB 090510, 090227B and 090228, all have additional power law components, in the 10 keV-10 MeV range, with very hard indices [19]. Fermi GBM can't by itself determine if there is a high energy cutoff for GRB 090227B and 090228. However it is clear that additional power laws are common in bright sGRBs. In our simulations we will assume that all sGRBs have an additional power law without cutoff with spectral index -1.6, consistent with evidence for sGRBs mentioned above.

The spectral index for the additional power law of LGRBs and sGRBs has the largest effect in our calculation. This is because we are extrapolating observations by Fermi LAT in the 0.1-10 GeV range up to hundreds of GeV.

3.2. Redshift distribution

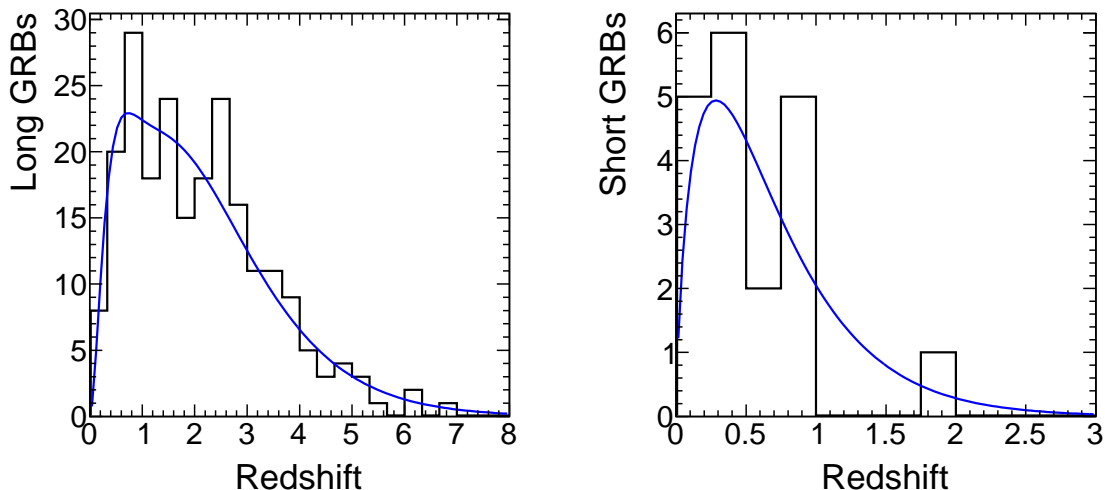


Figure 2: Redshift distribution for long (left) and short (right) GRBs. The curve shown is a function fitted to the data. LGRB data was collected from the online Swift catalog [20] See appendix for details on the selection of sGRBs.

E-pair production of the VHE GRB spectrum with extra-galactic background light results in a cutoff of the spectrum. This effect is redshift dependent, with higher redshifts resulting in a lower cutoff value. In our simulations we have parameterized the redshift distribution for both LGRBs and sGRBs.

For LGRBs we have used bursts of $T_{90} > 2$ s in the online Swift catalog [20]. The list of LGRBs was collected in March 2013. We exclude GRBs of $z \leq 0.1$ as they may be a separate population of very low luminosity GRBs that we are not trying to describe here. We find 223 LGRBs. The redshift distribution is fitted with an ad hoc function shown in figure 2. This is the very same function used for the calculation of the GRB rate in CTA [14], but fit parameters are different, as more LGRBs were used in the fit presented here.

Using a combination of the online Swift catalog [20] and other sources, we find 19 sGRBs with redshift measurements. An ad hoc function has been used to fit the distribution of sGRBs and is shown in figure 2. The list of sGRBs with redshift that we have used may be found in the appendix.

In our model we simulate GRBs of $z \geq 0.1$ and extend the spectrum at Earth up to a maximum of 1 TeV. These two choices are consistent as 1 TeV is approximately the cutoff expected for $z = 0.1$. Because the rate of GRBs of both types is very low below $z=0.1$, this choice of minimum redshift and maximum energy of the spectrum does not have a significant impact in our calculations. To calculate the effect of EBL attenuation and cutoff we use the 2009 model by Gilmore et al. [21], which is based on a semi-analytic treatment of galaxy formation and evolution and predicts a UV-optical EBL flux level similar to that seen in recent observationally-motivated models and galaxy survey data.

3.3. T_{90} distribution for LGRBs

As described in section § 2, we will assume that HAWC searches for VHE emission in a window of width equal to T_{90} as measured by GBM. We have parameterized the LGRB duration as using Fermi GBM's 2 year catalog [17]. The distribution of T_{90} is well described by a log-normal function. Figure 3 shows the data from the Fermi GBM 2 year catalog and the fit we have used.

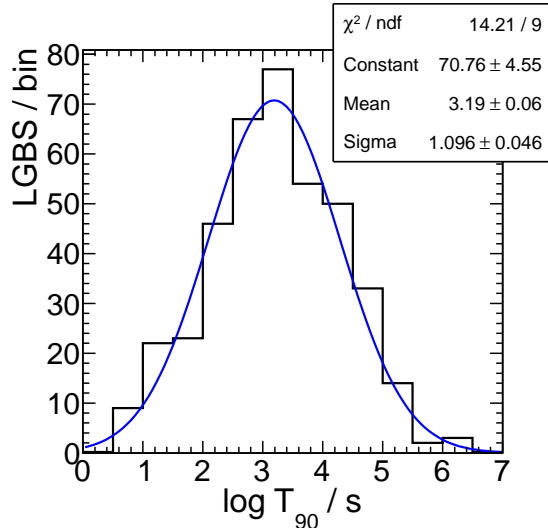


Figure 3: Distribution of T_{90} as measured for Fermi GBM in the 2 year catalog [17]. The fit is a log-normal distribution. A χ^2 of 14.2 with 9 degrees of freedom has a p-value of 0.115.

4. Detection rate in HAWC

Using the model described above and using interpolations of HAWC's effective area and parameterization of the background, we have calculated the GRB detection rate in HAWC. We find that sGRBs have a detection rate of 1.4 sGRB/yr (0.15 sGRB/yr) in the main DAQ (scaler DAQ). Figure 4 shows the distribution

of sGRBs as detected by Fermi GBM as well as HAWC with the main and scaler DAQs. We find that 90% of the sGRBs detected by the main DAQ (scaler DAQ) have a GBM fluence above 3.5×10^{-7} erg.cm $^{-2}$ (1.7×10^{-6} erg.cm $^{-2}$). This corroborates that our result is only modestly affected by the GBM trigger threshold. We also find that 90% of the sGRBs detected by the main DAQ (scaler DAQ) have a redshift of $z \leq 1.3$ ($z \leq 1.4$). Finally 90% of the sGRBs detected by the main DAQ (scaler DAQ) have a zenith of $\theta \leq 28^\circ$ (31°). We also find that all GRBs that can be detected with HAWC scalars are detected by the main DAQ.

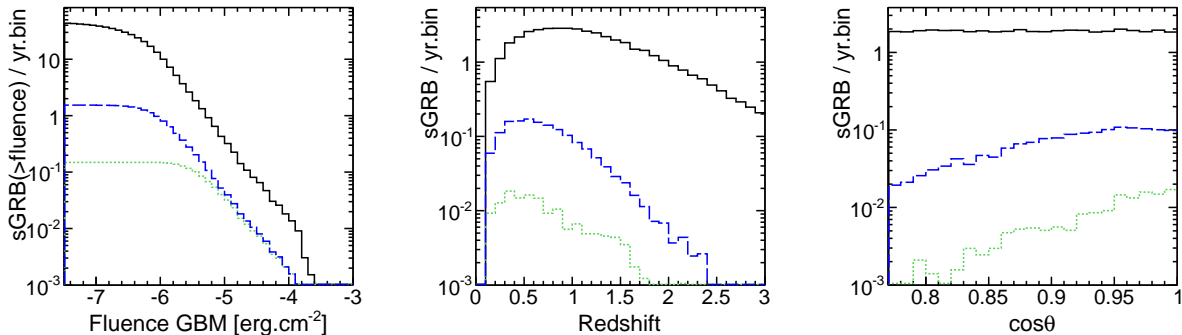


Figure 4: The three panels show the simulated distributions of short GRBs/yr detectable by Fermi GBM (black-solid lines) in fluence, redshift and zenith. The blue-dashed lines are GRBs detected by HAWC using the main DAQ, with default parameters. The green-dotted lines correspond to the scaler DAQ.

For LGRBs we find that the scaler DAQ has very poor prospects and we can't calculate it reliably with the simulated statistics of pseudo-GRBs, so we don't report the results here. For the main DAQ the detection rate of LGRBs is 0.25 GRB/yr. Figure 5 shows the distribution of LGRBs as detected by Fermi GBM as well as HAWC with the main DAQ. We find that 90% of the LGRBs detected by the main DAQ have a GBM fluence above 7×10^{-6} erg.cm $^{-2}$. We also find that 90% of the sGRBs detected by the main DAQ have a redshift of $z \leq 1.1$. Finally 90% of the sGRBs detected by the main DAQ have an elevation of $\theta \leq 32^\circ$.

For both types of GRBs we have estimated the energy range of photons that contribute to $> 5\sigma$ detection. For the main DAQ 90% of the photons detected from a typical GRB are in the ≈ 50 -500 GeV. For scalars the range is ≈ 6 -200 GeV. This is a reflection of the different energy sensitivity of each of the two systems.

For both types of GRBs we find what is reasonably expected: bright GBM GRBs, with small redshift and high elevation are the ones with best prospect for detection by HAWC.

Since the GRB spectrum may be cutoff at energies that are below the EBL cutoff, we have simulated a universal cutoff for all GRBs in the GRB reference frame. We have used cutoffs from 100 GeV to 500 GeV. Results are summarized in Table 1. For both main DAQ and scaler DAQ, the rate is reduced by half if the universal cutoff is somewhere between 200 and 300 GeV in the GRB reference frame.

5. > 10 GeV detection rate in Fermi LAT

To test whether the model describe here is reasonable, we have tested it against Fermi LAT. We have used our model to calculate the rate of GRBs with at least one photon above 10 GeV in Fermi LAT. We assume that the astrophysical backgrounds at 10 GeV and higher are virtually zero. We use the effective area at 10 GeV as a function of incidence angle that has been published by the Fermi LAT collaboration [22]. We also assume the effective area is constant as a function of energy above 10 GeV for all incidence angles.

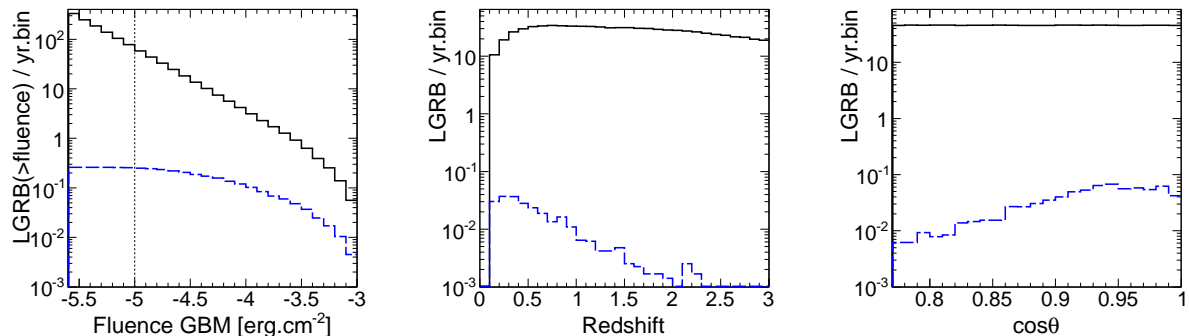


Figure 5: The three panels show the simulated distributions of long GRBs/yr detectable by Fermi GBM (black-solid lines) in fluence, redshift and zenith . The blue-dashed lines are GRBs detected by HAWC using the main DAQ, with default parameters. The green-dotted lines correspond the scaler DAQ.

Cutoff	main DAQ sGRB /yr	Scaler sGRB /yr	main DAQ LGRB /yr
n/a	1.4	0.15	0.25
500 GeV	1.3	0.12	0.22
400 GeV	1.2	0.11	0.20
300 GeV	0.97	0.10	0.15
200 GeV	0.54	0.07	0.08
150 GeV	0.27	0.05	0.04
100 GeV	0.07	0.02	0.01

Table 1: GRB rate with HAWC as a function of a universal cutoff in the GRB reference frame.

We find a rate of sGRBs of 0.26 sGRB/year and an LGRB rate of 1.2 LGRBs/year. As of the time of writing, Fermi LAT has been in operation for 4.7 years and has detected one sGRB above 10 GeV (GRB 090510), in agreement with our model. In the same time period LAT has detected 6 LGRBs above 10 GeV, also in agreement with our calculation.

For sGRBs we find that LAT should detect > 10 GeV photons for GBM fluence above $5 \times 10^{-6} \text{ erg} \cdot \text{cm}^{-2}$. For LGRBs, we find that LAT should detect > 10 GeV photons for a GBM fluence above $6 \times 10^{-5} \text{ erg} \cdot \text{cm}^{-2}$. Both these thresholds are not sharp, instead they depend on the angle of incidence in Fermi LAT.

Our calculation of the rate of GRBs in Fermi LAT above 10 GeV is very simplistic. We ignore multiple effects. For example, in normal operations Fermi LAT points away from Earth, but if a GRB alert is issued by GBM, then the satellite may be re-pointed so that Earth's limb could partially fall in the field of view of LAT. This would tend to increase the rate of GRBs seen above 10 GeV by LAT.

6. Discussion

Observations by Fermi LAT unequivocally show that GRBs produce VHE photons. But the observed sample of GRBs that produce high energy photons is very limited and with a wide variety of characteristics. In trying to describe the 1 GeV-1 TeV emission by GRBs, assumptions about spectral shape must be made and the spectrum must be extrapolated in energy over a few orders of magnitude. The calculations performed here are critically sensitive to the choice of extrapolation. A cautionary tale of predictions that depend on extrapolations is the pre-launch calculation of the GRB rate in Fermi LAT [23] which were overestimated. Nevertheless our model is consistent with current observations, save of the fraction of LGRBs that have an additional power law in the spectrum. We corroborated our model with respect to GRB observations by Fermi LAT and we found good agreement. If we assume that only one third of LGRBs have an additional power law, then the total GRB rate in HAWC is reduced to 1.51 GRBs/yr. Because both sGRBs detected

GRB	Redshift	GBM T_{90} (s)	References
050509B	0.2248	0.03	[24, 25]
050709	0.16	0.22	[26, 27]
050724	0.258	3.	[28, 29]
050813	1.8	0.6	[30, 31]
051221A	0.5464	1.4	[32, 33]
060502B	0.287	0.128	[34, 35]
061006	0.4377	0.42	[36, 37]
061201	0.111	2.	[38, 39]
061217	0.827	0.4	[40, 37]
070429B	0.902	0.5	[41, 42]
070714B	0.904	3.	[43, 44]
070724A	0.457	0.4	[45, 46]
070809	0.2187	2.	[47, 48]
071227	0.384	1.8	[49, 50]
080905	0.1218	0.6	[51, 52]
090510	0.903	0.5	[53, 54]
100117A	0.92	0.4	[55, 56]
100206A	0.41	0.13	[57, 58]
101219A	0.718	0.6	[59, 60]

Table 2: List of short-hard GRBs used to determine the redshift distribution

with high signal to noise ratio by Fermi LAT have an additional power law, we don't have good knowledge of the fraction of sGRBs that do have these power law. It is a critical assumption of our model that additional hard power laws are very common in short-hard GRBs.

We find that HAWC is most sensitive to short-hard GRBs. In our model we assume that half the VHE fluence is in temporal coincidence with Fermi GBM, from which it follows that HAWC is most sensitive in the prompt phase of the GRB. Interestingly the rate of short-hard GRBs in HAWC is higher than the rate in Fermi LAT above 10 GeV. Interestingly the rate of short-hard GRBs in HAWC is higher than the rate in Fermi LAT above 10 GeV. It is also worth noting that the subpopulation of GRBs visible to HAWC is almost entirely separate from the population predicted to be accessible to CTA in [14], as the latter will almost exclusively detect LGRBs.

The detection rate of GRBs in HAWC can be as high as 1.65 GRBs/year. The rate is lower if the spectrum has cutoffs at energies lower than that expected due to extra-galactic background light. A lower detection rate than the one presented here should allow HAWC to constrain the high energy spectral index, search for high energy cutoff and/or the fraction of GRBs with additional power law components.

Acknowledgments

IT acknowledges support by NSF grant PHY-1205807. RCG acknowledges support from a Fermi Guest Investigator Grant.

Appendix - Short-Hard GRBs.

Table 2 has been compiled from Swift's database [20] and from individual GCN circulars. At first list was drafted by selecting GRBs with a duration $T_{90} < 2$ s. The GCN and refereed publications for each GRB was reviewed to exclude potential long-soft GRBs with $T_{90} < 2$ s. We also include two GRBs that have the characteristics of short-hard bursts, even though they have a duration of ≈ 3 s.

References

- [1] S. Zhu et al., GCN Circ. 14471 (2013)
- [2] C.A. Meegan et al., ApJ. 702 (2009) 791
- [3] N. Gehrels, et al., ApJ. 611 (2004) 1005
- [4] M. Ruffert & H.T. Janka, A.&A. 344 (1999) 573-606
- [5] S. Rosswog, E Ramirez-Ruiz, M.B. Davies, MNRAS. 345 (2003) 1077-1090
- [6] K.Z. Stanek et al., ApJ. 591 (2003) L17-L20
- [7] A.A. Abdo et al., Science 323 (2009) 1688-1693
- [8] M. Ackermann et al., ApJ. 716 (2010) 1178-1190
- [9] Abdo A.A. et al., ApJ. 706 (2009) L138-L144
- [10] M. Ackermann et al., ApJ. 729 (2011) 114
- [11] M. Ackermann et al., 2013, Submitted to ApJ. Suppl. arXiv:1303.2908
- [12] D. Band et al., ApJ. 413 (1993) 281
- [13] V.A. Acciari et al., ApJ. 743 (2011) 62
- [14] R.C. Gilmore et al., Exp. Astron. (2012), doi:10.1007/s10686-012-9316-z
- [15] A.U. Abeysekera et al., Astropart. Phys. 35 (2012) 641-650
- [16] S. Vernetto, Astropart. Phys. 13 (2000) 75-86
- [17] W.S. Paciesas et al., ApJ. Suppl. 199 (2012) 18
- [18] A.A. Abdo et al., ApJ. 712 (2010) 558
- [19] S. Guiriec et al., ApJ. 725 (2010) 225
- [20] heasarc.nasa.gov/docs/swift/archive/grb_table/
- [21] R.C. Gilmore et al., MNRAS. 399 (2009) 1694-1708
- [22] www.slac.stanford.edu/exp/glast/groups/canda/lat_Performance.htm
- [23] B.L. Dingus, AIP Conf. Proc. 662 (2003) 240
- [24] B.D. Barthelmy et al., GCN Circ. 3385 (2005)
- [25] J.S. Bloom et al., ApJ. 638 (2006) 354-368
- [26] M. Boer et al., GCN Circ. 3653 (2005)
- [27] D.B. Fox et al., Nature. 437 (2005) 845
- [28] H. Krimm et al., GCN Circ. 3667 (2005)
- [29] J.X. Prochaska et al., GCN Circ. 3700 (2005)
- [30] G. Sato et al., GCN Circ. 3793 (2005)
- [31] E. Berger AIP Conf. Proc. 836 (2006) 33
- [32] J. Cummings et al., GCN Circ. 4365 (2005)
- [33] A.M. Soderberg et al., ApJ. 650 (2006) 261-271
- [34] E. Troja et al., GCN Circ. 5055 (2006)
- [35] J.S. Bloom et al., ApJ. 654 (2007) 878-884
- [36] Y. Urata et al., GCN Circ. 5717 (2006)
- [37] E. Berger et al., ApJ 664 (2007) 1000-1010
- [38] F.E. Marshall et al., GCN Circ. 5881 (2006)
- [39] G. Stratta et al., AIP. Conf.Proc. 1000 (2008) 297-300
- [40] Barthelmy S.D. et al., 2006, GCN Circ. 5926
- [41] J. Tueller et al., GCN Circ. 6365 (2007)
- [42] S.B. Cenko et al., arXiv:0802.0874
- [43] Racusin J.L et al., GCN Circ. 6620 (2007)
- [44] J. F. Graham et al., ApJ. 698 (2009) 16201629
- [45] A. Parsons et al., GCN Circ. 6656 (2007)
- [46] A. Cucchiara et al., GCN Circ. 6665 (2007)
- [47] F.E. Marshall et al., GCN Circ. 6728 (2007)
- [48] D.A. Perley et al., GCN Circ. 7889 (2007)
- [49] G. Sato et al., GCN Circ. 7148 (2007)
- [50] E. Berger et al., GCN Circ. 7154 (2007)
- [51] C. Pagani et al., GCN Circ. 8180 (2008)
- [52] A. Rowlinson et al., MNRAS. 408 (2010) 383-391
- [53] E.A. Hoversten et al., GCN Circ. 9331 (2009)
- [54] A. Rau et al., GCN Circ. 9353 (2009)
- [55] M. De Pasquale et al., GCN Circ. 10336 (2010)
- [56] W. Fong, arXiv:1012.4009
- [57] D. Palmer et al., GCN Circ. 10376 (2010)
- [58] S.B. Cenko et al., GCN Circ 10389 (2010)
- [59] J.A. Kennea et al., CGN Circ. 11461 (2010)
- [60] R. Chornock et al., GCN Circ. 11518 (2010)